47. Arief Adsorption

by Susila Arita

Submission date: 08-Mar-2020 03:56PM (UTC+0700)
Submission ID: 1271400766
File name: 47._Arief_Adsorption.pdf (379.71K)
Word count: 5505
Character count: 27265

Copyright © 2019 American Scientific Publishers
All rights reserved
Printed in the United States of America

Journal of
Computational and Theoretical Nanoscience
Vol. 16, 1–8, 2019

Adsorption Kinetic of Mn(II) Ions in Synthetic Acid Mine Water Using Calcium Carbide Residue as an Adsorbents

Muhammad Arief Karim[1,*], Subriyer Nasir[2], Susila Arita Rachman[2], and Novia[2]

[1] Chemical Engineering Department, Faculty of Engineering, Muhammadiyah University Palembang
Jl. Jendral Ahmad Yani 13 Ulu Palembang, 30263, Indonesia
[2] Chemical Engineering Department, Faculty of Engineering Sriwijaya University Jl. Raya Indralaya – Prabumulih KM. 32 Indralaya 30662

This investigation concentrated on diminishing the centralization of Mn(II) particles in manufactured corrosive mine water by the adsorption strategy utilizing calcium carbide buildups as an adsorbent. The adsorption procedure was examined utilizing 100 mL of arrangement of engineered corrosive mine with differing pH of 2.5 to 5 and weight of calcium carbide buildup from 2.5 to 7.5 g. The blend was mixed utilizing a shaker with speed of 200 rpm for 180 minutes with contact time ranges (5, 10, 20, 30, 40, 50, 60, 90, 120, 150, and 180 minutes) and the underlying centralizations of Mn(II) of between 20 to 100 mg/L. The outcomes demonstrated that adsorption limit of adsorbent increments with expanding of starting grouping of Mn(II) particles in the arrangement. The Freundlich isotherm model matches the observational information. Adsorption energy demonstrated that this response pursues the pseudo-second adsorption model. The most extreme adsorption limit with respect to Mn(II) as arrangement is 41.67 mg/g at pH 5. The outcomes additionally shown that calcium carbide buildups are reasonable for adsorbing Mn(II) particles from fluid arrangements.

Keywords: Adsorption, Kinetic, Calcium Carbide Residue, Mn Metal.

RESEARCH ARTICLE

1. INTRODUCTION

The mining business is commonly a noteworthy supporter of corrosive mine seepage (AMD). Corrosive mine water that requirements genuine consideration when released into water bodies. One of the broke down metals in corrosive mine water (AMD) is manganese ions (Mn(II)) which causes dark brown shade of the water when reaching with air [1], and will be dangerous when the centralization of Mn(II) particles disintegrated in water more prominent than 0.02 mg/L [2]. Manganese metals particle in corrosive mine water are found in different structures, both intricate and natural mixes [3]. Manganese particles are hard to expel from AMD since they precipitated when the pH is over 10 [4]. Accordingly, it is a need to diminish the manganese particles so the water is ok for condition. A few innovations have been created for killing corrosive mine water, including the adsorption procedure, particle trade, invert assimilation dissolvable extraction, flocculation and film detachment [5], electrochemistry [6], electrodialysis [7], just as ultrafiltration innovation, electrolysis, and extraction [8]. Among these techniques, adsorption is financially and in fact straight forward, moderately simple to work, basic structure, does not cause unsafe and exceptionally powerful in adsorbing substantial metals particles [9, 10].

Enacted carbon is a standout amongst the best adsorbents, yet it requires costly expenses in the actuation procedure. In this way, it is important to search for the ease adsorbent. One potential material that can be created as a modest and, effectively accessible is strong waste from the welding business utilizes calcium carbide called calcium carbide buildup. As per Jiang [11], calcium carbide buildup has a high range of pH somewhere in the range of 12.84 and 13.2, explicit gravity of 2.32, explicit surface territory is 24.664 m^2/g. This examination planned to research the capability of calcium carbide buildup as an adsorbent for diminishing manganese (Mn) content from AMW with the goal that it is appropriate to be discarded to the accepting water body.

2. MATERIALS AND METHOD

2.1. Preparation of the Adsorbent Material

Calcium carbide residue (CCR) from a neighborhood welding in Palembang, South Sumatra, Indonesia was utilized as an adsorbent. In the wake of cleaning and absorbing distillate water medium-term and dried normally in sunshine, and sieved into 80 work of molecule estimate. The adsorbent was made into tablets structure with a

*Author to whom correspondence should be addressed.

thickness of 2 mm and width of 3 mm and warmed utilizing the broiler at 150 °C for 120 minutes. The normal load of one tablet dry adsorbent is 0.5 g [12].

Manufactured corrosive mine water was set up by dissolving $M_n[SO]_{4.4}H_2O$ into refined water to acquire a centralization of 100 mg/L and put in a bottle with limit of 40 L at room temperature. To get the ideal focus dilution, a solution of $H_2[SO]_4$ 0, 1 N was included request to alter the pH of arrangement and filtered using Whatman channel paper No. 1.

2.2. Batch Adsorption Experiments

The process of adsorption of Mn(II) ions was carried out using a batch method at room temperature with initial concentrations of 20, 40, 60, 80, 100 mg/L and the weight of adsorbent calcium carbide residue were 2, 5 and 7.5 g, mixed into 100 mL of synthetic AMW solution. The mixture was stirred using shaker with a speed of 200 rpm for 180 minutes and the sample is taken periodically from 5 to 180 minutes.

2.3. Adsorption Capacity and Removal Efficiency

The amount of reduction in Mn(II) ions per mass of adsorbent at a certain time (q_t) is calculated based on the formula in Eq. (1) [13].

$$q_e = \frac{(C_0 - C_t) * V}{m} \tag{1}$$

The percentage of adsorption of heavy metals iron (II) ions from solution is calculated using the following equation [14]:

$$\text{Adsorption } (\%) = \frac{(C_o - C_t)}{C_o} \times 100\% \tag{2}$$

Where, q_t is the adsorbent retention limit at time t; C_o is the underlying grouping of the metal in arrangement (mg/l); C_t is the convergence of metal in arrangement after time t (mg/l); V is the volume of arrangement (L) and m is the mass of the adsorbent in arrangement (g).

The Langmuir adsorption condition is a standout amongst the most widely recognized isotherm conditions used to show balance information in a strong fluid framework. This condition applies to the monolayer surface with various indistinguishable locales disseminated homogeneously on the outside of the adsorbent. The general type of the Langmuir condition is communicated in a straight structure, as pursues [15, 16].

$$\frac{C_e}{q_e} = \frac{1}{bq_m} + \frac{C_e}{q_m} \tag{3}$$

Where b and q_m: are Langmuir constants which are identified with the adsorption rate (L/mg) and adsorption limit (mg/g).

The Freundlich isotherm adsorption model depicts a heterogeneous adsorption process superficially with a non-uniform warmth adsorption dissemination [17]. As indicated by the Freundlich isotherm adsorption model, the mass of adsorbate ingested per mass of adsorbent can be communicated as a component of solute fixation, C_e. The direct type of the Freundlich isotherm adsorption technique is detailed as condition (4):

$$\log q_e = \log K_f + \frac{1}{n}(\log C_e) \tag{4}$$

Where K_f and n are Freundlich constants. To decide K_f and n, every one of them utilizes a direct relapse estimation of the capture and incline diagram ($\log q_e$) versus ($\log C_e$) while the connection R2 gives a sign of the model picked [18].

By utilizing the straight condition come nearer from the chart of Langmuir and Freundlich isotherms, we can know the adsorption limit of CCR adsorbent. Assurance of Langmuir adsorption isoterm was gotten by making a bend of the connection between the harmony focus in the fluid stage (C_e) to the strong stage balance fixation (C_e/q_e), for Freundlich adsorption isotherm acquired by charting the connection between log C_e with log q_e.

2.4. Adsorption Kinetics

Study of adsorption energy is significant in light of the fact that it can give data about procedure elements, for example, adsorption rate, living arrangement time, and motor parameters. In this way, dynamic investigations helping in assess the appropriateness of materials utilized as potential adsorbents in expelling poisons from arrangements [2]. Exploratory information testing for the adsorption response model should be possible with pseudo first request models and pseudo second request models. The pseudo first request model is the condition model that is most generally utilized for the procedure of adsorption of solids from arrangements. This model is an adsorption speed model dependent on adsorption limit [19]. Ho and McKay [20] clarified that some first-request pseudo conditions were utilized to recognize dynamic conditions dependent on the adsorption limit of the centralization of adsorbate in arrangement. The condition of the pseudo first request model can be displayed as pursues.

$$\log(q_e - q_t) = \log q_e - \frac{k_1}{2{,}303}t \tag{5}$$

By plotting $\log(q_e - q_t)$ on t, the correlation value of R^2 will be obtained and the first order (k_1) adsorption reaction rate value from the graph slope obtained. Whereas the pseudo-second-order kinetic model given by [20] is defined as.

$$\frac{t}{q_t} = \frac{1}{k_2(q_e)^2} + \frac{1}{q_e}t \tag{6}$$

Where q_t is the number of metal ions absorbed in equilibrium conditions (mg/g); (k_2) is the pseudo-second-order rate constant kinetic applied (mg/g/h), plot t/q_t with t will give a linear line.

3. RESULTS AND DISCUSSION

Portrayal of CCR adsorbent

Morphological portrayal of the adsorbent was completed to decide the compound substance and physical and concoction properties of CCR. Portrayal was done utilizing SEM-EDX (Filtering Electron Magnifying lens Dispersive X-Beam Analisis). SEM-EDX is one sort of electron magnifying lens that can create high goals from the picture of an example surface. The portrayal of adsorbent was likewise done by infrared spectroscopy or normally called Fourier Change Infrared (FTIR) which means to decide the utilitarian gatherings of mixes contained in CCR as appeared in Figure 1.

Figures 1(a) and (b), demonstrate that there are morphological changes on the outside of CCR when adsorption process. This demonstrating there is an accelerated of Mn(II) particles in the adsorbent surface. This outcome is likewise upheld by the EDX (Vitality Dispersive X-Beam) investigation which is available the components in the CCR before and after the adsorption process. Characterization utilizing EDX to acquire data on the substance of components found in the CCR, as appeared in the range of portrayal in Figures 2(a) and (b), and Table I.

From Figures 2(a) and (b), and Table I, it very well may be seen that the CCR before being utilized as adsorbent was dominate by calcium, and after the adsorption procedure the calcium substance diminishes from 52, 83 to 30.95 wt%. While the substance of Mn(II) particles exist after the adsorption procedure with a measure of 5.57 wt%.

Table I. The composition of the CCR before and after adsorption.

Component/composition (%)			
Before adsorption		After adsorption	
Elements	(wt.%)	Elements	(wt.%)
Ca	52.83	Ca	30.95
Au	24.30	Au	25.26
O	16.56	O	28.15
C	3.76	C	8.27
Al	1.56	Al	0.79
Si	0.98	Si	1.01
		Mn	5.57
Total	100	Total	100

Portrayal of utilitarian gatherings of the CCR was additionally done by FTIR Spectrophotometer to recognize the natural mixes, both subjectively and quantitatively (Figs. 3(a and b)). The investigation is finished by taking a gander at the state of the range and tops that show the kind of practical gathering controlled by the compound. The consequences of FTIR portrayal of practical gatherings of the CCRs acquired with a recurrence scope of 4000–500 cm^{-1} are demonstrated by a diagram of the connection between the wavelength and Transmittance, as appeared in Figures 3(a) and (b).

In view of the consequences of FTIR when adsorption as appeared in Figures 3(a) and (b). A portion of the pinnacles saw in the range demonstrate that the CCRs have a useful gathering crest which can tie cations. At the wavelength of 3637.9 cm^{-1} and 3362.1 cm^{-1} compares to the extending of the hydroxyl (-Goodness) work within the vibration which shows the nearness of COO- symmetric carboxyl gatherings, suggesting the nearness of kaolinite elements [21, 22]. While at the stature of the band tops 28775, 2817.97 and 2512.2 cm^{-1} speaking to flexural (-Goodness) vibrations and furthermore as

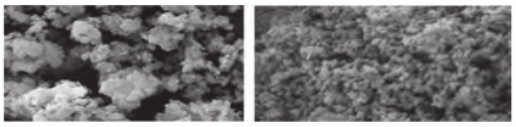

(a) (b)

Fig. 1. (a) Surface morphology of adsorbent the CCR before adsorption (magnificent of 5000 times). (b) Surface morphology of adsorbent the CCR after adsorption (magnificent of 5000 times).

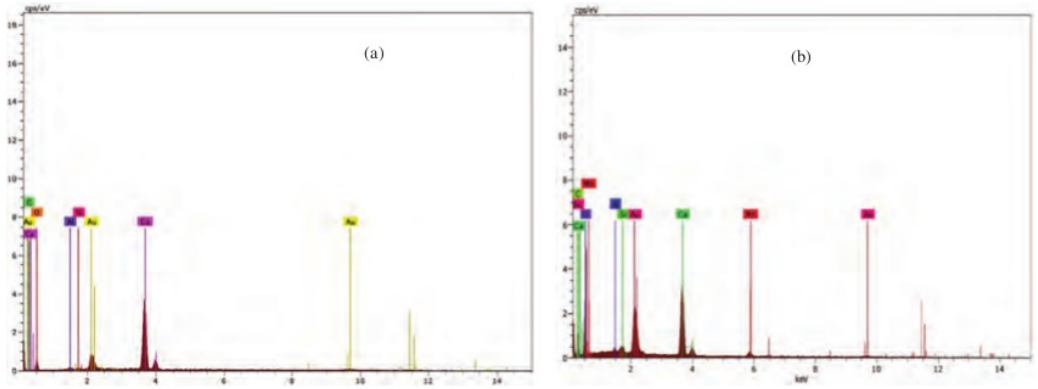

Fig. 2. (a) Characteristic spectrum of CCR before adsorption. (b) Characteristic spectrum of CCR after adsorption.

RESEARCH ARTICLE

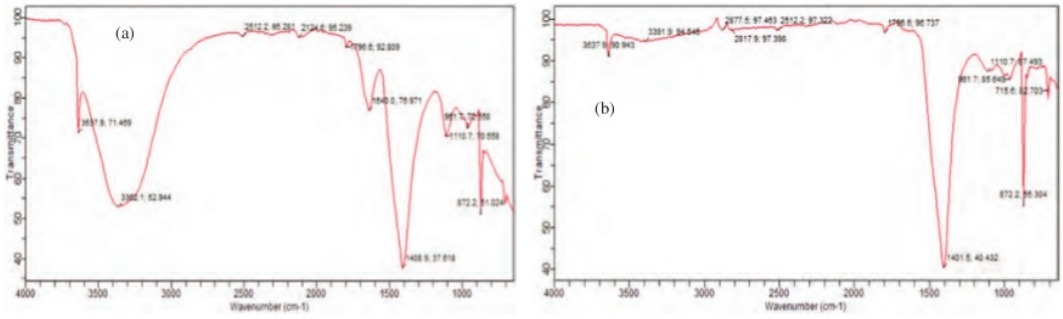

Fig. 3. (a) FTIR of CCR before adsorption. (b) FT-IR of CCR after adsorption.

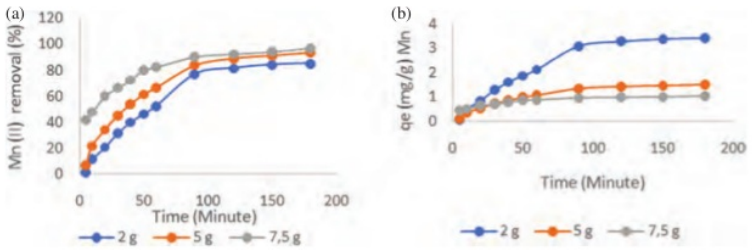

Fig. 4. (a) Effect of mass of adsorbent to percent reduction in Mn(II) ions. (b) Effect of mass of adsorbent to the adsorption capacity of Mn(II) ions.

RESEARCH ARTICLE

symmetrical COO extend vibrations, showing the nearness of hydroxyl [23, 24], then sharp crests at 1401.5 and 1110.7 cm^{-1} were because of Si–O strain vibrations, for retention band statures 961.7 and 872.2 identified with flexural vibrations demonstrating the presence of Al–O gathering [25], and there is another band as high as 715 cm^{-1} related with vibration Mn–O extending in manganite [26].

3.1. Effect of the Adsorbent Period

The information got plot the connection between the measure of metal Mn(II) particles adsorbed to time and plot the measure of metal expulsion of Mn(II) particles to the season of every time of the CCR, as appeared in Figure 4.

Figure 4(a) the level of the CCR take-up is exceptionally quick in expelling Mn(II) particles and increments with expanding mass of the CCR. The adsorption limit of the CCRs achieves immersion stage at an hour and a half nearly for all mass of carbide calcium buildup. The underlying reduction of Mn(II) is quick because of the expansion in the outside of the adsorbent and along these lines delivers a progressively dynamic site for Mn adsorption. Figure 4(b) demonstrates the impact of contact time and adsorption limit of the CCR. During the principal hour, the adsorption limit demonstrated a fast increment and afterward gradually expanded until it achieved the ideal time at 100 minutes. The level of evacuation is higher toward the beginning of this trial because of the accessible

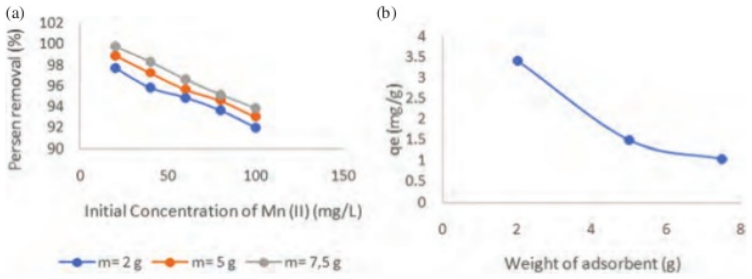

Fig. 5. (a) Effect of initial concentration on percent adsorption of Mn(II). (b) Effect of mass of adsorbent on absorption power.

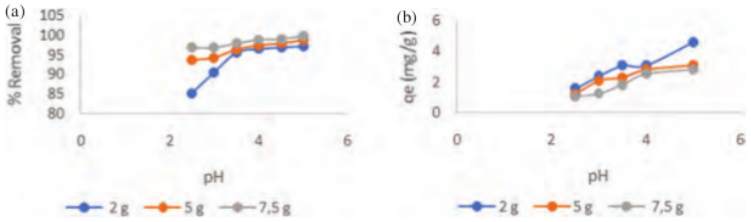

Fig. 6. (a) Effect of pH on the adsorption percentage. (b) Effect of absorption rate on pH.

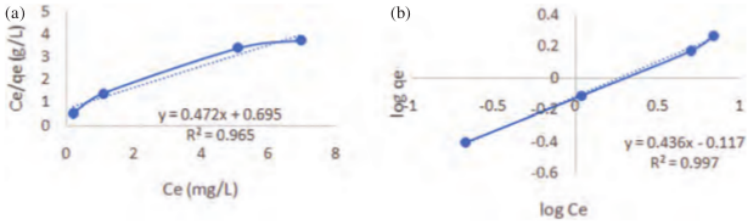

Fig. 7. Langmuir and Freundlich plot graphs for Mn adsorption with adsorbent calcium carbide residues. (a) Langmuir model. (b) Freundlich model.

surface territory of the CCR for retention of metal Mn(II) particles.

3.2. Effect of Mn(II) Ion Concentration

The impact of beginning convergence of Mn(II) arrangement was examined with different mass carbide calcium buildups, in particular 2, 5 and 7.5 gr. The calcium carbide buildup put into 100 ml of Mn(II) arrangement with fluctuating fixations, between 20 to 100 mg/L with an unsettling rate of 200 rpm. The impact of the underlying fixation on the adsorption of Mn(II) particles utilizing the CCR for 180 minutes is appeared in Figure 5.

In Figures 5(a) or (b), it tends to be seen that the level of adsorption of Mn(II) particles diminishes altogether with an expanding beginning convergence of Mn(II) particles in arrangement. At the underlying centralization of 20 mg/L for the mass of adsorbent carbide calcium buildup 2 gr, the level of adsorption of Mn(II) was 97.7% diminishing to 91.98% at the underlying convergence of Mn(II) particles of 100 mg/L. While for the mass of adsorbent carbide calcium buildup 5 gr, there was a reduction from 98.93% to 93.03%. For mass, the leftover carbide calcium is 7.5 gr, the level of adsorption of Mn(II) particles drops from 99.8% to 93.9%. In Figure 7(b) it tends to be seen that the more noteworthy the mass of the adsorbent, the more prominent the capacity of lingering calcium carbide to adsorb metal Mn(II) particles.

3.3. Effect of pH on Mn(II) Ion Removal

The effect of pH in this study was studied in the range of 2.5; 3.5 and 5 at room temperature. The initial concentration of Mn(II) ion solution was set at 80 mg/L, stirring speed 200 rpm, contact time of 160 minutes and mass variation of adsorbent 2, 5 and 7.5 g. The results of the analysis obtained are shown in Figure 6.

In Figure 6 it very well may be seen that the expansion in the underlying pH of the arrangement can build the measure of Mn(II) particles consumed by the remaining calcium carbide. The level of manganese expulsion at pH 2.5–5 is moderately high at 97.25% for the adsorbent load of 2 g, 98.73% for mass adsorbent 5 g and 99.9% for mass adsorbent 7.5 g. While the adsorption limit (q_e) of Mn metal by the most extreme carbide calcium buildup happens in the mass of 2 gr adsorbent with an underlying pH of 5.0 arrangement, which is equivalent to 5.6 mg/g and the least at 7.5 g adsorbent mass with the underlying pH of arrangement 2, 5, which is equivalent to 1.03 mg/g. In these conditions, the pH of the blend in the adsorption procedure goes up to 10, 5. This is because of the exceptionally high pH of the underlying carbide

Table II. Parameters of adsorption of Mn ions as a result of linearization of the equation of the Langmuir and Freundlich adsorption models.

	Langmuir					Freundlich			
Time (minute)	Linear equations	q_0	R^2	K_L	R_L	Linear equations	R^2	K_F	$1/n$
180	$Y = 0{,}4723X + 0{,}695$	2,117	0,9652	0,223	0,01	$Y = 0{,}4368X - 0{,}1173$	0,997	0,763	0,437

RESEARCH ARTICLE

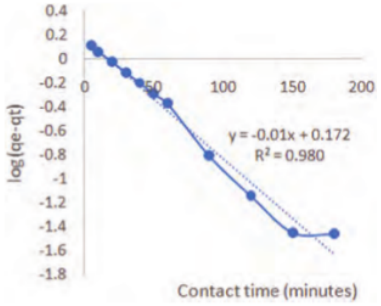

Fig. 8. Relationship log $(q_e - q_t)$ curve versus t.

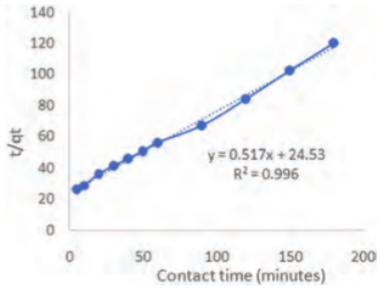

Fig. 9. Relationship curve t/q_t versus t.

calcium buildup, which is 12.5. At the high pH estimation of the blend, the grouping of hydrogen particles as contenders is lower, causing an expansion in the quantity of metal particles Mn(II) assimilated from the arrangement [27, 28]. At low pH beneath 4 the quantity of H+ particles are extremely enormous so that there is rivalry between Mn(II) particles and Hydrogen particles to keep the dynamic adsorbent gathering, this challenge causes disturbance of the retention procedure of Mn(II) particles with the goal that the measure of substantial metal particles adsorbed is low [28].

3.4. Equilibrium Adsorption Isotherms

Model Langmuir and Freundlich adsorption isotherm are utilized to depict a gathering of information acquired at a specific fixation scope of perceptions. The perceptions in this examination led by the underlying centralization of the particle Mn(II) 80 mg/L and mass of adsorbent remaining calcium carbide 5 g contact time 180 minutes. To decide the suitable isotherm condition on research by taking a gander at the relationship coefficient (R2) got from the direct diagram of every condition. A relationship coefficient near one can be said to pursue the sort of adsorption isotherms of the adsorption isotherm condition, as appeared in Figure 7.

From Figure 7 the price of the Langmuir and Freundlich constants can be calculated from the linear C_e/q_e versus C_e plot and log q_e versus log C_e. As shown in Table II.

The most extreme adsorption limit (q_o) of Table II above, at the contact time of 180 minutes as per the Langmuir model is 2.117 mg/g and the R2 worth is 0.9652 and the consistent cost of Langmuir partiality (K_L) is 0.223 L/mg and (R_L) of 0.01 (generally excellent) on the grounds that it is littler than 1 $(0 < R_L < 1)$. While for the Freundlich isotherm model the cost of R2 is acquired at 0.9974 and the cost of Freundlich consistent (K_F) is 0.763 and the force esteem (1/n) is 0.4368. From Table II, it very well may be presumed that the adsorption isotherm model in decreasing the grouping of Mn(II) particles pursues the Freundlich isotherm model. The Freundlich adsorption isotherm model demonstrates a direct connection between the quantity of substances adsorbed per gram of adsorbent in the adsorption procedure of Mn(II) by the CCR, with the condition $q_e = 0{,}736C\_e\text{^}0{,}4368$, this implies the isotherm design in engrossing Mn metal particles (II) by the adsorbent of calcium carbide strong waste, because of the dynamic side of the strong waste surface calcium carbide is multilayer, with irregular dispersion and liking over heterogeneous surfaces.

3.5. Study of Adsorption Kinetics

The dynamic model utilized in this examination is pseudo-first request, pseudo-second request. Both of these dynamic models are ordinarily used to decide the request of adsorption energy [19]. To discover how the system, viability and productivity and how quick the adsorption procedure of Mn(II) particles happens utilizing adsorbent the CCRs, it is important to think about pseudo-first-request and two-pseudo request energy. Perceptions were done at the underlying convergence of 80 mg/L and the mass of adsorbent carbide buildups 5 g with contact times of 5 to 180 minutes, information acquired by communicating conditions 4 and 5. Insertion after effects of adsorption of metal particle Mn(II) between logs $(q_e - q_t)$ to t appeared in Figure 8 and between t/q_t versus t in Figure 9. The parameter esteems and connection coefficients got

Table III. Parameters and linearity equation of one and two pseudo-order kinetics models.

	Pseudo kinetic model first order				Pseudo kinetic model second order			
Massa RCC	Linear equation	q_e	R^2	k_1	Linear equation	q_e	R^2	k_2
2	$y = -0{,}0158x + 0{,}8824$	7,628	0,911	0,125	$y = 0{,}1869x + 17{,}653$	5,350	0,9920	0,0019
5	$y = -0{,}01x + 0{,}1724$	1,487	0,981	0,023	$y = 0{,}5179x + 24{,}532$	1,931	0,9962	0,0109
7,5	$y = -0{,}0119x - 0{,}0726$	0,846	0,943	0,027	$y = 0{,}8622x + 18{,}326$	1,159	0,996	0,0406

RESEARCH ARTICLE

from counts dependent on Figures 8 and 9, as in Table III.

From the relationship coefficient esteems are displayed in Table III. In light of the coefficient of assurance (R2) got from the third time of the adsorbent remaining calcium carbide is connected, the mass of 5 grams of the most great. The estimation of the relationship coefficient (R^2) most near 1, i.e., = 0.9962 by the quantity of particle Mn(II) adsorbed at harmony (q_e) is 1.931 mg/g, with the pace of the energy of k_2 to be specific 0.0109, gr. mg/minute. R2 qualities got from particle adsorption of Mn(II) by the CCR following the model of the pseudo-second-request energy. As indicated by Defeat [29], and Huang [30] when adsorption models pursue the model of pseudo-second-request energy, it tends to be sorted adsorption process which happens between the CCR and particle Mn(II) is synthetic adsorption (chemisorption) [31–33].

4. CONCLUSION

Adsorption limit and adsorption proficiency are expanded with expanding pH and diminished with expanding in weight of adsorbent.The adsorption limit of the outside of the CCRs for Mn(II) particles increments with an expansion in pH and introductory convergence of the arrangement of Mn(II) ions [34].

Testing the Freundlich and Langmuir isotherm models for test information demonstrates that: the Freundlich isotherm model matches the exploratory outcomes. The Freundlich adsorption isotherm model demonstrates a direct connection between the measure of adsorbed substance per gr adsorbent in the adsorption procedure of Mn(II) with the condition $q_e = 0{,}736C\_e$^0,4368.

The use of pseudo-first-request energy and pseudo-second-request dynamic models demonstrates that the adsorption of Mn(II) particles on the CCRs, most intently pursues the second-request pseudo energy model.

References

1. Stephen Siwila, Chopa Chota, Kumbu Yambani, Dingase Sampa, Amon Siangalichi, Niza Ndawa and Gabriel Tambwe, **2017**. Design of a small-scale iron and manganese removal system for Copperbelt University's borehole water. *J. Environ. Geol., 1*(1), pp.24–30.
2. Silva, A.M., Cunha, E.C., Silva, F.D. and Leao, V.A., **2012**. Treatment of high-manganese mine water with limestone and sodium carbonate. *J. Clean Prod., 29–30*, pp.11–19.
3. Roccaro, P., Barone, C., Mancini, C. and Vagliasindi, F.G., **2007**. Removal of manganese from water supplies intended for human consumption: A case study. *Desalination, 210*, pp.205–214.
4. Earle, J. and Callaghan, T., **1998**. Impacts of mine drainage on aquatic life, water uses, and man-made structures. In *Coal Mine Drainage Prediction and Pollution Prevention in Pennsylvania*, edited by K. B. C. Brady, M. W. Smith, and J. Schueck, Department of Environmental Protection, Harrisburg, PA.
5. Kwon, J.S., Yun, S.T., Leea, J.H., Kim, S.O. and Jo, H.Y., **2010**. Removal of divalent heavy metals (Cd, Cu, Pb, and Zn) and arsenic (III) from aqueous solutions using scoria: Kinetics and equilibria of sorption. *Journal of Hazardous Materials, 174*, pp.307–313.
6. Luptakova, A., Ubaldini, S., Fornari, P. and Macingova, E., **2012**. Physical–chemical and biological-chemical methods for treatment of acid mine drainage. *Chemical Engineering Transactions, 28*, pp.115–120.
7. Buzzi, D.C., Viegas, L.S., Rodrigues, M.A.S., Bernardes, A.M. and Tenório, J.A.S., **2013**. Water recovery from acid mine drainage by electrodialysis. *Minerals Engineering, 40*, pp.82–89.
8. Motsi, T., Rowson, N.A. and Simmons, M.J.H., **2011**. Kinetic studies of the removal of heavy metals from acid mine drainage by natural zeolite. *International Journal of Mineral Processing, 101*, pp.42–49.
9. Das, B., Mondal, N.K., Bhaumik, R., Roy, P., Pal, K.C. and Das, C.R., **2013**. Removal of copper from aqueous solution using alluvial soil of Indian origin: Equilibrium, kinetic and thermodynamic study. *J. Mater. Environ. Sci., 4*, pp.392–408.
10. Karthikeyan, T., Rajgopal, S. and Miranda, L.R., **2005**. Chromium (VI) adsorption from aqueous solution by Hevea brasilinesis sawdust activated carbon. *Journal of Hazardous Materials, 124*, pp.192–199.
11. Jiang, N.J., Du, Y.J., Liu, S.Y., Wei, M.L., Horpibulsuk, S. and Arulrajah, A., **2016**. Multi-scale laboratory evaluation of the physical, mechanical, and microstructural properties of soft highway subgrade soil stabilized with calcium carbide residue. *Can. Geotech. J., 53*(3), pp.373–383.
12. Muhammad Arief Karim, Subriyer Nasir, Susila Arita Rachman and Novia, **2019**. Reduction of Iron (II) Ions in Synthetic Acidic Wastewater Containing Ferro Sulphate Using Calcium Carbide Residu, *AIP Conference Proceedings*, Vol. 2085, p.0200025.
13. Vijayaraghavan, K., Padmesh, T.V.N., Palanivelu, K. and Velan, M., **2006**. Biosorption of nickel (II) ions onto Sargassum wightii: Application of two-parameter and three parameter isotherm models. *Journal of Hazardous Materials, B133*, pp.304–308.
14. Erdem, E., Karapinar, N. and Donat, R., **2004**. The removal of heavy metal cations by natural zeolites. *Journal of Colloid and Interface Science, 280*(2), pp.309–314.
15. Nleya, Y., **2016**. Removal of Toxic Metals and Recovery of Acid from Acid Mine Drainage Using Acid Retardation and Asorption Processes, Sammri Hydrometallurgy Symposium, University of Cape Town, South Africa.
16. Nwabanne, J.T. and Igbokwe, P.K., **2012**. Adsorption performance of packed bed column for the removal of lead (ii) using oil palm fibre. *International Journal of Applied Science and Technology, 2*(5), pp.108–117.
17. Günay, A., Arslankaya, E. and Tosun, I., **2007**. Lead removal from aqueous solution by natural and pretreated clinoptilolite: Adsorption equilibrium and kinetics. *Journal of Hazardous Materials, 146*, pp.362–371.
18. Kumar, P.S., Vincent, C., Kirthika, K. and Kumar, K.S., **2010**. Kinetics and equilibrium studies of Pb^{2+} ion removal from aqueous solutions by use of nano-silversol-coated activated carbon. *Brazilian Journal of Chemical Engineering, 27*(02), pp.339–346.
19. Qiu, H., Lv, L., Pan, B.C., Zhang, Q.J., Zhang, W.M. and Zhang, Q.X., **2009**. Critical review in adsorption kinetic models. *Journal of Zhejiang University-Science A, 10*(5), pp.716–724.
20. Ho, Y.S. and McKay, G., **2000**. The kinetics of sorption of divalent metal ions onto sphagnum moss peat. *Water Research, 34*(3), pp.735–742.
21. Wang, J.P., Feng, H.M. and Yu, H.Q., **2007**. Analysis of adsorption characteristics of 2.4-dichlorophenol from aqueous solutions by activated carbon fiber. *Journal of Hazardous Materials, 144*, pp.200–207.
22. Ekosse, G.E., **2011**. Fourier transform infrared spectrophotometry and X-ray powder diffractometry as complementary techniques in characterizing clay size fraction of kaolin. *J. Environ. Sci., 23*(3), pp.404–11.
23. Huang, K. and Zhu, H., **2013**. Removal of Pb (II) from aqueous solution by adsorption on chemically modified muskmelon peel. *Environ. Sci. Pollut. Res., 20*(7), pp.4424–34.

24. Li, Y., Xia, B., Zhao, Q., Liu, F., Zhang, P. and Du, Q., **2014**. l of copper ions from aqueous solution by calcium alginate immobilized kaolin. *J. Environ. Sci., 23*(3), pp.404–11.

25. Vempati, R.K., Mollah, M.Y.A., Reddy, G.R. and Cocke, D.L., **1996**. Intercalation of kaolinite under hydrothermal conditions. *J. Mater. Sci., 31*, pp.1255–1259.

26. Sharma, P.K. and Whittingham, M.S., **2001**. The role of tetraethyl ammonium hydroxide on the phase determination and electrical properties of γ-MnOOH synthesized by hydrothermal. *Materials Letters, 48*, pp.319–323.

27. Myroslav, Sprynskyy, Boguslaw, Buszewski, Artur, Terzyk, P., Jacek, Namiesnik, **2006**. Study of the selection mechanism of heavy metal (Pb2+, Cu2+, Ni2+ and Cd2+) adsorption on clinoptilolite. *J. Colloid Interface Sci., 304*, pp.21–28.

28. Motsi, T., Rowson, N.A. and Simmons, M.J.H., **2009**. Adsorption of heavy metals from acid mine drainage by natural zeolite. *International Journal of Mineral Processing, 92*, pp.42–48.

29. Rout, P.R., Bhunia, P. and dan Dash, R.R., **2014**. Modeling isotherms, kinetics, and understanding the mechanism of phosphate adsorption onto A solid waste: Ground burn patties. *Journal of Environmental Chemical Engineering, 10*, p.1016.

30. Huang, W.Y., Li, D., Liu, Z.Q., Tao, Q., Zhu, Y., Yang, J. and Zang, Y.M., **2014**. Kinetics, isotherm, thermodynamic, and adsorption mechanism of La(OH)3-modified exfoliated vermiculites as highly efficient phosphate adsorbents. *Chemical Engineering Journal, 236*, pp.191–201.

31. Amanlou, M. and Mostafavi, S.M., **2017**. *In sillico* screening to aim computational efficient inhibitors of caspase-9 by ligand-based pharmacophore modeling. *Medbiotech. Journal, 01*(01), pp.34–41.

32. Mostafavi, S.M., Bagherzadeh, K. and Amanlou, M., **2017**. A new attempt to introduce efficient inhibitors for caspas-9 according to structure-based pharmacophore screening strategy and molecular dynamics simulations. *Medbiotech Journal, 01*(01), pp.1–8.

33. Heidary, S., Imani, M. and Mostafavi, S.M., **2017**. A validated and rapid HPLC method for quantification of human serum albumin in interferon beta-1a biopharmaceutical formulation. *Medbiotech Journal, 01*(01), pp.29–33.

34. Shahriyar, Tavousi Tafreshi, Mohammad Reza, and Nikoomanesh, **2013**. Study of the effect of the numbers of middle piers (bases) in the numbers of effective modes in seismic evaluation of bridge. *UCT Journal of Research in Science, Engineering and Technology*, (4), pp.01–05.

Received: 1 January 2019. Accepted: 11 March 2019.

RESEARCH ARTICLE

47. Arief Adsorption

ORIGINALITY REPORT

2%	0%	1%	2%
SIMILARITY INDEX	INTERNET SOURCES	PUBLICATIONS	STUDENT PAPERS

MATCH ALL SOURCES (ONLY SELECTED SOURCE PRINTED)

1%

★ P. Senthil Kumar, A.S.L. Sai Deepthi, R. Bharani, C. Prabhakaran. " Adsorption of Cu(II), Cd(II) and Ni(II) ions from aqueous solution by unmodified seeds ", European Journal of Environmental and Civil Engineering, 2013

Publication

Exclude quotes	On	Exclude matches	< 1%
Exclude bibliography	On		